NJC

PAPER

Check for updates

Cite this: *New J. Chem.*, 2018, **42**, 16021

Structural and bonding properties of $BS^{-/0}$ and $BS_3^{-/0}$†

Li-Juan Zhao,[a] Xi-Ling Xu,*[a] Hong-Guang Xu,[a] Gang Feng[b] and Wei-Jun Zheng*[ac]

Received 17th April 2018,
Accepted 26th August 2018

DOI: 10.1039/c8nj01835a

rsc.li/njc

Anion photoelectron spectroscopy and theoretical calculations were used to investigate the structural, electronic, and bonding properties of BS^- and BS_3^-. Vibrationally resolved photoelectron spectra of BS^- at 355 nm and 266 nm were obtained. The electron affinity of BS is determined to be 2.32 ± 0.05 eV. The stretching vibrational frequencies of BS^- and BS were measured to be 968 cm^{-1} and 1210 cm^{-1}, respectively. The results indicate that the B–S bond in $BS^{-/0}$ can be characterized as a triple bond. The B–S bond in neutral BS is stronger than that in anionic BS^-. The most stable isomer of BS_3^- has a C_{2v} symmetric planar structure with the B atom at the center interacting with the three S atoms, while that of neutral BS_3 has a S–B–S–S bent structure.

1. Introduction

Boron has unique bonding characters due to its electron deficiency. It prefers to form multi-center σ bonds and π bonds. Typical examples are all-boron α-sheet[1] and all-boron fullerene,[2] in which the bonds are multi-center two-electron bonds. In the last few decades, species consisting of electron-deficient boron and electron-rich atoms such as boron oxides have received great attention. It is found that B and O atoms can form a very stable BO moiety, which is isovalent to CN. Theoretical results indicated that the BO group is a radical similar to an Au atom.[3,4] New types of multi-center bonds were identified including 3c–4e hyperbonds[5–8] and 4c–4e o-bonds.[5,6,9] In addition, some boron oxides such as $B_3O_3(BO)_3$ were predicted to be inorganic analogues of benzene or other carbon hydrides by quantum chemical calculations.[10] Moreover, the B_4 units in $B_n(BO)_2^-$ (n = 5–12) clusters were assigned to be the building blocks of boron nanoribbons and were also proposed as precursors of the low-dimensional boron nanostructures.[11]

Similar to boron oxides, boron sulfides were also investigated extensively. Zeeman measured and analyzed the three extensive band systems of BS generated by electric discharge on boron trisulfide (B_2S_3).[12] The bond dissociation energies of BS and BS_2 were studied by mass spectrometry technique and it was found that the gaseous BS has a rather high dissociation energy, indicating that it has a high bond order.[13] The ESR spectra of the BS molecule were measured at 4 K.[14] The isotropic shifts and spin-rotation interaction constant for BS were measured by microwave spectroscopy.[15,16] The spin–orbit coupling, spectroscopic constants, and transition properties of BS were analyzed *via ab initio* calculations.[17,18] The absorption spectrum of BS_2 was measured in neon matrices[19] and the laser-induced fluorescence spectrum of BS_2 was measured[20–22] in the gas phase. A strong pseudo Jahn–Teller effect was identified in BS_2 according to the infrared spectra and theoretical calculations.[23] The theoretical results suggested that BS_2 can be used as building blocks for new materials such as hyperhalogens.[24,25] $B_2S_3^+$, $B_2S_2^+$, and BS_2^+ were investigated by mass spectrometry and infrared emission spectroscopy.[26] Mass spectroscopic studies on high molecular weight boron sulfides suggested that BS_2 and B_2S_3 were monomers of polymerization and their vaporization behavior was explored.[27–30] The crystal structures of $(BS_2)_n$, $(B_2S_3)_n$ and B_8S_{16} ("inorganic porphine") were characterized by X-ray diffraction analysis.[31–33] Furthermore, BS_3^{3-}, $B_2S_4^{2-}$, $B_2S_5^{2-}$, and $B_3S_6^{3-}$ were found to exist as discrete anions in their metal boron sulfides.[34] Theoretical calculations suggested that $B_2(BS)_2^-$, $B_2(BS)_2^{2-}$, and $B(BS)_4^-$ were analogous to their corresponding boron hydrides $B_2H_2^-$, $B_2H_2^{2-}$, and BH_4^-, and revealed that $B_6S_6^{0/-/2-}$ were boron sulfide analogues of naphthalene.[35–37] The anion photoelectron spectroscopy study of boron sulfides is very rare except that the electron affinity, bonding, and superhalogen properties of BS_2^- were explored by anion photoelectron spectroscopy.[38] In this paper, we report combined anion photoelectron spectroscopy and theoretical studies on the structural, electronic, and bonding properties of BS^- and BS_3^- clusters.

[a] *Beijing National Laboratory for Molecular Sciences, State Key Laboratory of Molecular Reaction Dynamics, Institute of Chemistry, Chinese Academy of Sciences, Beijing 100190, China. E-mail: xlxu@iccas.ac.cn, zhengwj@iccas.ac.cn; Fax: +86 10 62563167; Tel: +86 10 62635054*

[b] *School of Chemistry and Chemical Engineering, Chongqing University, Chongqing 401331, China*

[c] *University of Chinese Academy of Sciences, Beijing 100049, China*

† Electronic supplementary information (ESI) available. See DOI: 10.1039/c8nj01835a

2. Experimental and theoretical methods

2.1 Experimental methods

The experiments were carried out on a home-built apparatus consisting of a linear time-of-flight (TOF) mass spectrometer and a magnetic-bottle photoelectron spectrometer.[39] Briefly, the BS^- and BS_3^- anions were produced by laser ablation of a rotating and translating boron–sulfur mixture disk target (13 mm diameter, a $^{11}B/S$ molar ratio of 1 : 1) with the second harmonic of a nanosecond Nd:YAG laser (Continuum Surelite II-10). The typical laser power used in this work was about 10 mJ per pulse. Helium carrier gas with about 4 atm backing pressure was allowed to expand through a pulsed valve (General Valve Series 9) over the target to cool the formed clusters. The generated clusters anions were analyzed using the time-of-flight mass spectrometer. The BS^- and BS_3^- anions were selected using a mass gate, decelerated using a momentum decelerator, and photodetached with the light beam of another Nd:YAG laser (Continuum Surelite II-10; 532 nm, 355 nm, or 266 nm). The photoelectrons produced were energy-analyzed using the magnetic-bottle photoelectron spectrometer. The photoelectron spectra were calibrated by using the spectra of Bi^-, Cs^-, Cu^-, and Au^- obtained under similar conditions. The resolution of the photoelectron spectrometer was about 40 meV at an electron kinetic energy of 1 eV.

2.2 Theoretical methods

The structures of the BS^- and BS_3^- anions as well as those of their corresponding neutral species were optimized using density functional theory (DFT) with the Becke three-parameter hybrid exchange functional combined with the Lee–Yang–Parr correlation functional (B3LYP)[40,41] and the augmented correlation-consistent polarized valence triple-zeta basis sets (aug-cc-pVTZ),[42] which are obtained from the EMSL basis set exchange[43] using the Gaussian 09 program package.[44] All the possible structural candidates were considered. Anions at singlet and triplet multiplicities as well as neutrals at the doublet and quadruplet multiplicities were optimized. Harmonic vibrational frequency analyses were carried out to make sure that the obtained structures were true local minima. Further, the *ab initio* single-reference coupled cluster theory with single, double, and non-iterative triple excitations (CCSD(T))[45–47] combined with the aug-cc-pVTZ basis set were then implemented using the Molpro 2012 software.[48] The T1 diagnostics of BS^- and BS_3^- are 0.021 and 0.015 at the CCSD(T) level, which indicates that the multiconfigurational character is not significant for BS^- and BS_3^-. The relative energies were used to estimate the vertical detachment energies (VDEs) and the adiabatic detachment energies (ADEs) of BS^- and BS_3^-, where the VDE is defined as the energy difference between the neutral and anion both at the equilibrium structure of the anion, whereas the ADE is the energy difference between the neutral and anion with the neutral relaxed to the nearest local minimum using the anionic structure as the initial structure. Molecular orbital (MO) analyses were conducted to explore their bonding characters. The Wiberg bond indices (WBI) were determined by natural bond orbital (NBO) analyses.[49]

3. Results

The photoelectron spectra of BS^- measured with 532 nm, 355 nm, and 266 nm photons are presented in Fig. 1. The simulated spectrum of BS^- is also displayed in Fig. 1. The simulated spectrum is generated based on the generalized Koopmans' theorem[50,51] and Franck–Condon (FC) simulation using the ezSpectrum program.[52] Fig. 2 shows the photoelectron spectrum of BS_3^- taken with 266 nm photons and its simulated density of states (DOS) spectrum. The calculated structures of the BS^- and BS_3^- anions as well as those of their corresponding neutrals are presented in Fig. 3 and Fig. S1 (ESI†). The theoretical ADEs and VDEs of the low-lying isomers of BS^- and BS_3^- obtained at the B3LYP and CCSD(T) levels are listed in Table 1 and Table S1 (ESI†) in comparison with the experimental ones.

3.1 BS^- and BS

As shown in Fig. 1, the 266 nm spectrum of BS^- has a few peaks between 2.30 and 3.00 eV. The onset of another feature above 4.20 eV is also observed in the 266 nm spectrum. The peaks between 2.30 and 3.00 eV are better resolved in the 355 nm spectrum into five peaks centered at 2.32, 2.47, 2.62, 2.77, and 2.92 eV with an energy gap of about 0.15 eV (1210 cm^{-1}). These peaks can be assigned to the vibrational progression related to the transition from the electronic ground state of BS^- to the

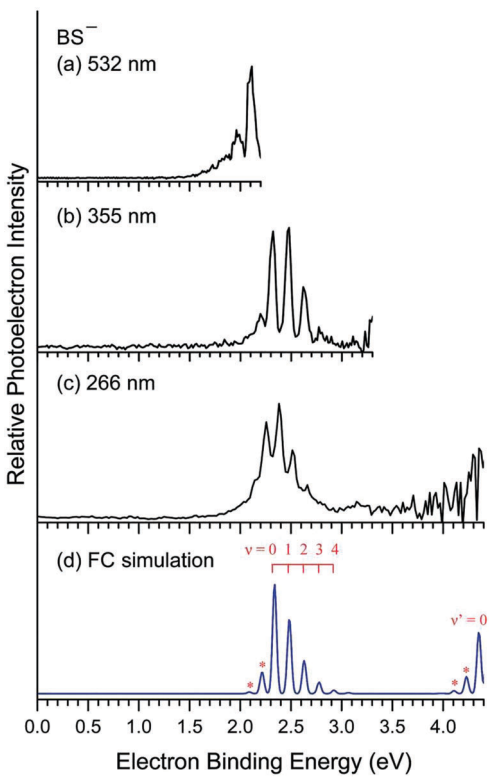

Fig. 1 Photoelectron spectra of BS^- measured with (a) 532 nm, (b) 355 nm, and (c) 266 nm photons and (d) the Franck–Condon (FC) simulation spectrum (blue line) at 1000 K. Each vibrational transition peak is fitted with a unit-area Gaussian function of 0.02 eV full width at half maximum (FWHM). The red vertical lines represent the vibrational resolved features. And the asterisks (*) stand for hot bands.

 This journal is © The Royal Society of Chemistry and the Centre National de la Recherche Scientifique 2018

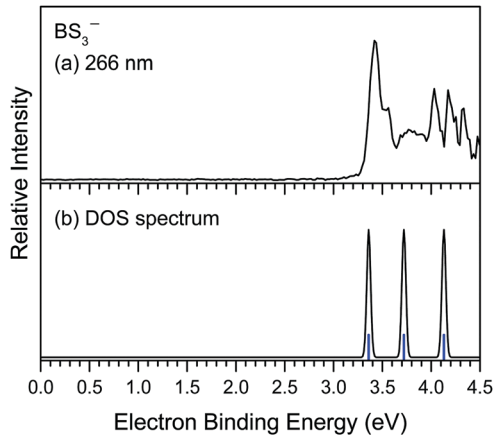

Fig. 2 Comparison of (a) photoelectron spectrum of BS_3^- measured with 266 nm photons and its (b) density of states (DOS) spectrum. The blue vertical lines are the theoretically simulated spectral lines. In the DOS simulation, the positions of the spectral lines are aligned with the HOMO and its two lower molecular orbitals. Each spectral line was fitted with a unit-area Gaussian function of 0.02 eV FWHM.

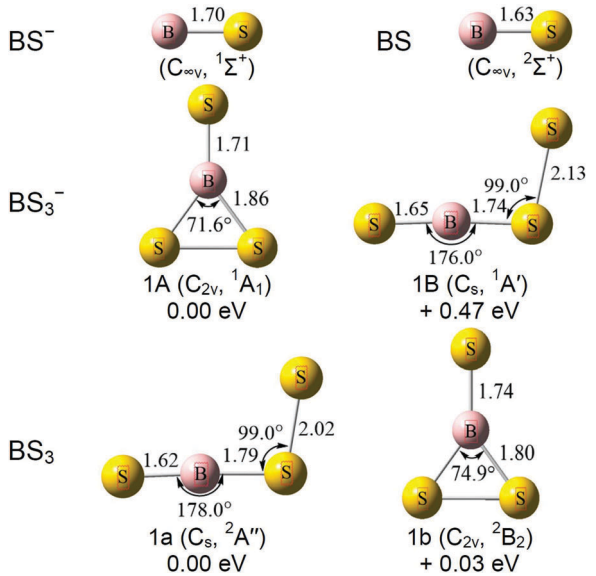

Fig. 3 Typical low-lying isomers of BS^- and BS_3^- as well as their corresponding neutrals. The electronic state, bond lengths (in Å) and bond angles are labeled. The relative energies to their most stable isomers obtained at the CCSD(T) level.

electronic ground state of neutral BS. In addition, there are two "hot bands" centered at 2.20 and 2.07 eV, which may result from the vibrational excited state of the BS^- anion. The spacing between the "hot band" at 2.20 eV and the first major peak is about 0.12 eV (968 cm^{-1}). The experimental ADE value of BS^- is estimated from the first major peak to be 2.32 eV, and its experimental VDE value is determined from the second major peak to be 2.47 eV.

BS^- is a closed shell species in a $^1\Sigma^+$ electronic state, while the electronic state of BS is $^2\Sigma^+$. The B–S bond distance of BS^- is calculated to be 1.70 Å. Its theoretical ADE/VDE values are 2.33/2.43 eV at the B3LYP level, and 2.28/2.38 eV at the CCSD(T) level, which are in good agreement with the experimental ones (2.32/2.47 eV). The calculated B–S bond distance of neutral BS is 1.63 Å, which is consistent with the previous theoretical value (1.62 Å).[17] The B–S bond distance of neutral BS is shorter than that of the BS^- anion by 0.07 Å, indicating that the electron removed is detached from an orbital with a somewhat antibonding character. The B–S stretching vibrational frequency of BS^- is calculated to be 989 cm^{-1} (~0.12 eV) at the B3LYP level and 987 cm^{-1} (~0.12 eV) at the CCSD(T) level, which are consistent with the energy spacing (0.12 eV) between the "hot band" at 2.20 eV and the first major peak at 2.32 eV. The B–S stretching vibrational frequency of BS is calculated to be 1180 cm^{-1} (0.146 eV) at the B3LYP level and 1172 cm^{-1} (0.145 eV) at the CCSD(T) level, which are in good agreement with the interval of the vibrational progression (1210 cm^{-1}) observed in the 355 nm spectrum in this work and the harmonic vibrational constant (ω_e, 1200 cm^{-1}) reported by Boggs.[17] The term energy of the first electronic excited state of BS ($^2\Pi$) is calculated to be 2.07 eV at the TD-B3LYP level, which is in agreement with the spectroscopic term reported previously.[17,53,54] The B–S bond length of the BS ($^2\Pi$) state is calculated to be 1.80 Å. The vibrational frequency of the BS ($^2\Pi$) state is about 747 cm^{-1}. Based on the term energy, the calculated VDE value of the first electronic excited state of BS ($^2\Pi$) at the TD-B3LYP level is 4.50 eV, which can explain why only the rising edge of this spectral feature is observed in the 266 nm spectrum.

To verify the assignment of the vibrational progression, the spectrum of BS^- was simulated and the VDEs of the ground and excited electronic states were determined by B3LYP and TD-B3LYP calculations. Then the vibrational progression of each electronic state was simulated with FC simulations at 1000 K, as shown in Fig. 1(d). It can be seen that the FC simulation

Table 1 The relative energies, ADEs and VDEs of the low-lying isomers of BS^- and BS_3^- obtained by theoretical calculations and a comparison with the experimental ADEs and VDEs

					ADE (eV)			VDE (eV)		
			ΔE (eV)		Theo.			Theo.		
Isomer			B3LYP	CCSD(T)	B3LYP	CCSD(T)	Expt.	B3LYP	CCSD(T)	Expt.
BS^-		$C_{\infty v}$, $^1\Sigma^+$			2.33	2.28	2.32(5)[a]	2.43	2.38	2.47(5)[a]
BS_3^-	1A	C_{2v}, $^1A_1$	0.00	0.00	3.31	3.37	3.34(5)[a]	3.36	3.44	3.42(5)[a]
	1B	C_s, $^1A'$	0.32	0.47	2.88	2.86		3.01	3.00	

[a] The numbers in the parentheses indicate the uncertainties of the experimental values in the last digits.

spectrum is in line with the 355 nm and 266 nm spectra. This indicates that the BS^- anions generated in our cluster source are relatively hot. The vibrational progression and hot bands of the $BS(X, {}^2\Sigma^+) \leftarrow BS^-(X, {}^1\Sigma^+)$ and $BS(A, {}^2\Pi) \leftarrow BS^-(X, {}^1\Sigma^+)$ transitions are assigned. For the first vibrational resolved feature, the $0 \leftarrow 0$ transition, which stands for the transition from the vibrational ground state of the BS^- anion to that of BS neutral, defines the ADE value of BS^- (the EA of BS). And the $0 \leftarrow 1$ transition determines the energy gap between the first major peak and its neighboring "hot band". And for the second feature, the transitions from the former two vibrational excited states of the BS^- anion to the vibrational ground state of $BS(A, {}^2\Pi)$ are also determined, which correspond to the weak peaks at above 4.00 eV due to the low detection efficiency.

In order to better understand the bonding characters of BS^-, molecular orbitals are analyzed. Some key valence molecular orbitals are shown in Fig. 4. According to the bonding analyses, BS^- has a $1\sigma^2 2\sigma^2 1\pi^4 3\sigma^2$ valence electronic configuration. The HOMO mainly from the B atom (2s, 51%; $2p_z$, 34%) has a slight anti-bonding character, which is consistent with the shorter bond distance of B–S in BS than that in BS^- by 0.07 Å and the larger stretching vibrational frequency in BS (1172 cm^{-1}) than that in BS^- (987 cm^{-1}) at the CCSD(T) level. The approximate Lewis presentation of BS^- is proposed and shown in Fig. 5. It can be seen from Fig. 5 that BS^- has a B≡S triple bond character and the B1 and S2 atoms each have a lone electron pair. The HOMO−3 (B: 13% 2s, 8% $2p_z$; S: 72% 3s, 2% $3p_z$) and degenerate HOMO−1s (B: 16% $2p_x$ or $2p_y$; S: 84% $3p_x$ or $3p_y$) constitute the σ and π orbitals of the B≡S triple bond. One electron detachment from the HOMO−1s indicates the bond weakening in the first electronic exited state (1.80 Å) of neutral BS, which is consistent with the bond length elongation by 0.10 Å as well as the vibrational frequency weakening (747 cm^{-1}) compared to that of the BS^- anion (987 cm^{-1}). For BS neutral, it is a radical and has a relatively stronger BS bond than that in the BS^- anion, which can also be characterized as a B≡S triple bond. The triple bond character of BS is in agreement with the bond dissociation energy of BS (4.29 eV) measured by Gingerich *et al.*[13] The Wiberg bond order of BS^- is calculated to be 1.97 and that of BS is calculated to be 2.30 at the B3LYP level, which are in agreement with their relative bond strengths although

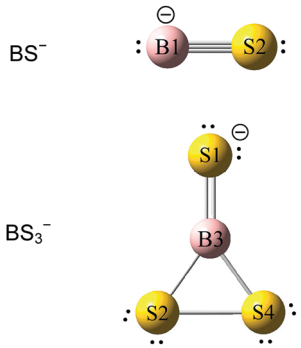

Fig. 5 Schematic Lewis presentations for BS^- and BS_3^-. Lone pair electrons as well as their negatively charged centers are labeled.

the bond orders are underestimated by the theory. The natural population atomic (NPA) charge analyses of $BS^{-/0}$ indicate that the electron is mainly detached from the B atom (0.61 e), as listed in Table 2, which is also consistent with the B atom dominated electron cloud distributed HOMO of BS^-.

Here we compare $BS^{-/0}$ with $BO^{-/0}$, which were investigated previously.[55] BS^- and BO^- are both closed shell species with a similar valence electronic configuration. Both BS^- and BO^- have one approximate triple bond. The vibrational frequency of BS (1210 cm^{-1}) is lower than that of BO (1935 cm^{-1}), and that of BS^- (968 cm^{-1}) is also lower than that of BO^- (1725 cm^{-1}). The bond distance of BS (1.63 Å) is longer than that of BO (1.20 Å), and that of BS^- (1.70 Å) is also longer than that of BO^- (1.23 Å). These indicate that the B–S bond in BS is weaker than the B–O bond in BO, which is also true for BS^- and BO^-. The first electronic excited state energy of BS (~2.07 eV) is lower than that of BO (2.96 eV), as determined by comparing their photoelectron spectra. The electron affinity of BS is measured to be 2.32 eV, which is lower than that of BO (2.51 eV). This is in line with the electronegativity order of the S and O atoms (χ_S (2.58) < χ_O (3.44)).

3.2 BS_3^- and BS_3

In Fig. 2, the spectrum of BS_3^- recorded with 266 nm photons has a relatively sharp peak at 3.42 eV and a shoulder at 3.56 eV, a broad band centered at about 3.80 eV, and three high electron

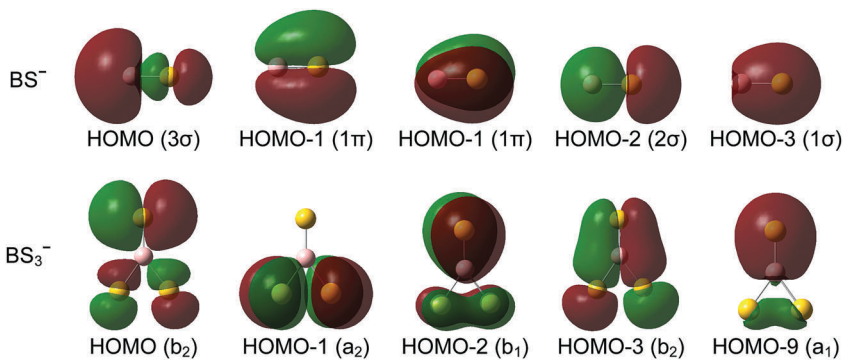

Fig. 4 Selected key valence molecular orbitals of BS^- and BS_3^-.

 This journal is © The Royal Society of Chemistry and the Centre National de la Recherche Scientifique 2018

Table 2 The natural population atomic (NPA) charges of $BS^{-/0}$ and $BS_3^{-/0}$ at the B3LYP level

Species	Atom	NPA charge	Species	Atom	NPA charge	Electron loss
BS^-	B1	−0.27	BS	B1	0.34	0.61
	S2	−0.73		S2	−0.34	0.39
BS_3^- 1A	S1	−0.54	BS_3 1b	S1	0.12	0.66
	S2	−0.22		S2	0.02	0.24
	B3	−0.02		B3	−0.16	−0.14
	S4	−0.22		S4	0.02	0.24
BS_3^- 1B	S1	−0.40	BS_3 1a	S1	−0.12	0.28
	S2	−0.11		S2	0.06	0.17
	B3	0.17		B3	0.12	−0.05
	S4	−0.66		S4	−0.06	0.60

binding energy peaks centered at 4.03, 4.17, and 4.32 eV. The experimental VDE of BS_3^- is determined to be 3.42 eV from the maximum of the first peak. Its experimental ADE is estimated to be 3.34 eV.

As shown in Fig. 3, two types of structures, planar and bent, for $BS_3^{-/0}$ were determined from our calculations. The ground state structure of the BS_3^- anion (1A) is a planar structure with a BS_2 three-membered ring, while that of BS_3 neutral is a sulfur–boron–sulfur–sulfur (S–B–S–S) bent structure (1a). The planar structure (1A) of the BS_3^- anion has a C_{2v} symmetry with the B atom at the center interacting with the three S atoms. The theoretical ADE and VDE values of the planar structure (1A) calculated at the B3LYP level (3.31 and 3.36 eV) and CCSD(T) level (3.37 and 3.44 eV) agree well with the experimental values (3.34 and 3.42 eV). The theoretical VDE values of the bent structure (1B) calculated at the B3LYP and CCSD(T) levels are 3.01 and 3.00 eV, which are much smaller than the experimental VDE value. From Fig. 2, we can see that the DOS spectrum of the planar structure is in line with the major peaks at 3.42, 3.80, and 4.05 eV in the experimental spectrum of BS_3^-. The shoulder and the other peaks in the experimental spectrum are due to the vibrational progressions of the corresponding neutral electronic excited states. Therefore, the planar structure (1A) is the most probable isomer detected in our experiments and the existence of the bent structure (1B) in the experiments can be ruled out.

BS_3^- has a closed-shell electronic structure with a $^1A_1$ electronic state. According to the bonding analyses, its approximate Lewis presentation is shown in Fig. 5. We can see that the central B3 atom forms one double bond with the S1 atom and two single bonds with the S2 and S4 atoms, forming one B3S2S4 three-membered ring. The HOMO−2 (S1: 75% $3p_x$; B3: 11% $2p_x$; S2: 7% $3p_x$; S4: 7% $3p_x$) and HOMO−9 (S1: 65% 3s; B3: 16% $2p_z$, 10% 2s) shown in Fig. 4 constitute the σ and π orbitals of the S1═B3 double bond. The NPA charge analyses indicate that the electrons are mainly removed from the S1 atom by 0.66 e for the planar structures of $BS_3^{-/0}$ (1A, 1b), which is consistent with the HOMO of BS_3^-, whose electron cloud is mainly located on the S1 atom (78% $3p_y$). And the S1–B3 bond distance increases very slightly, which further confirms the mainly non-bonding character of the HOMO of BS_3^-. The NPA charge analyses also suggest that for the S–B–S–S bent structures of $BS_3^{-/0}$ (1B, 1a) electrons are mainly detached from the S4 atom by 0.60 e.

4. Conclusions

The structural, electronic, and bonding properties of BS^- and BS_3^- were investigated by anion photoelectron spectroscopy and theoretical calculations. Their neutral counterparts were also studied by theoretical calculations. The electron affinity of BS is measured to be 2.32 ± 0.05 eV. It is found the $BS^{-/0}$ has a triple bond character. BS^- has a longer bond length than neutral BS. The ground state structure of BS_3^- is a C_{2v} symmetric planar structure, while that of BS_3 is a S–B–S–S bent structure. These results indicate that the extra electron can affect the geometric structures of these clusters.

Conflicts of interest

There are no conflicts to declare.

Acknowledgements

This work was supported by the National Natural Science Foundation of China (Grant No. 21303214) and the Chinese Academy of Sciences (Grant No. QYZDB-SSW-SLH024). The theoretical calculations were conducted using ScGrid and DeepComp 7000 at the Supercomputing Center, Computer Network Information Center of Chinese Academy of Sciences.

References

1 H. Tang and S. Ismail-Beigi, *Phys. Rev. Lett.*, 2007, **99**, 115501.
2 H.-J. Zhai, Y.-F. Zhao, W.-L. Li, Q. Chen, H. Bai, H.-S. Hu, Z. A. Piazza, W.-J. Tian, H.-G. Lu and Y.-B. Wu, *Nat. Chem.*, 2014, **6**, 727–731.
3 Q. Chen, H. Bai, H.-J. Zhai, S.-D. Li and L.-S. Wang, *J. Chem. Phys.*, 2013, **139**, 044308.
4 H.-J. Zhai, C.-Q. Miao, S.-D. Li and L.-S. Wang, *J. Phys. Chem. A*, 2010, **114**, 12155–12161.
5 L.-J. Zhao, W.-J. Tian, T. Ou, H.-G. Xu, G. Feng, X.-L. Xu, H.-J. Zhai, S.-D. Li and W.-J. Zheng, *J. Chem. Phys.*, 2016, **144**, 124301.
6 W.-J. Tian, L.-J. Zhao, Q. Chen, T. Ou, H.-G. Xu, W.-J. Zheng, H.-J. Zhai and S.-D. Li, *J. Chem. Phys.*, 2015, **142**, 134305.
7 W.-J. Tian, X.-R. You, D.-Z. Li, T. Ou, Q. Chen, H.-J. Zhai and S.-D. Li, *J. Chem. Phys.*, 2015, **143**, 064303.
8 W.-J. Tian, H.-G. Xu, X.-Y. Kong, Q. Chen, W.-J. Zheng, H.-J. Zhai and S.-D. Li, *Phys. Chem. Chem. Phys.*, 2014, **16**, 5129–5136.
9 Q. Chen, H. Lu, H.-J. Zhai and S.-D. Li, *Phys. Chem. Chem. Phys.*, 2014, **16**, 7274–7279.
10 D.-Z. Li, H. Bai, Q. Chen, H. Lu, H.-J. Zhai and S.-D. Li, *J. Chem. Phys.*, 2013, **138**, 244304.
11 H.-J. Zhai, Q. Chen, H. Bai, H.-G. Lu, W.-L. Li, S.-D. Li and L.-S. Wang, *J. Chem. Phys.*, 2013, **139**, 174301.
12 P. B. Zeeman, *Phys. Rev.*, 1950, **80**, 902.
13 K. A. Gingerich, *Chem. Commun.*, 1970, 580.
14 J. M. Brom and W. Weltner, *J. Chem. Phys.*, 1972, **57**, 3379–3384.

15 M. Tanimoto, S. Saito and S. Yamamoto, *J. Chem. Phys.*, 1988, **88**, 2296–2299.
16 S. Gopal and G. Lakshminarayana, *Pramana*, 1986, **28**, 159–165.
17 X. Yang and J. E. Boggs, *Chem. Phys. Lett.*, 2005, **410**, 269–274.
18 J. M. Sennesal, J. M. Robbe and J. Schamps, *Chem. Phys.*, 1981, **55**, 49–56.
19 J. M. Brom Jr. and W. Weltner Jr., *J. Mol. Spectrosc.*, 1973, **45**, 82–98.
20 S.-G. He, D. J. Clouthier, A. G. Adam and D. W. Tokaryk, *J. Chem. Phys.*, 2005, **122**, 194314.
21 S.-G. He and D. J. Clouthier, *J. Chem. Phys.*, 2004, **120**, 4258–4262.
22 S.-G. He, C. J. Evans and D. J. Clouthier, *J. Chem. Phys.*, 2003, **119**, 2047–2056.
23 J. Zhao, W. J. Yu, T. F. Huang and X. F. Wang, *Chin. J. Chem. Phys.*, 2017, **30**, 678–684.
24 L.-P. Ding, X.-Y. Kuang, P. Shao, M.-M. Zhong and Y.-R. Zhao, *RSC Adv.*, 2013, **3**, 15449–15456.
25 J. V. Ortiz, *Chem. Phys. Lett.*, 1993, **214**, 467–472.
26 A. Sommer, P. N. Walsh and D. White, *J. Chem. Phys.*, 1960, **33**, 296–297.
27 H.-Y. Chen and P. W. Gilles, *J. Phys. Chem.*, 1972, **76**, 2035–2038.
28 H.-Y. Chen and P. W. Gilles, *J. Am. Chem. Soc.*, 1970, **92**, 2309–2312.
29 F. T. Greene and P. W. Gilles, *J. Am. Chem. Soc.*, 1964, **86**, 3964–3969.
30 F. T. Greene and P. W. Gilles, *J. Am. Chem. Soc.*, 1962, **84**, 3598–3599.
31 B. Krebs, *Angew. Chem., Int. Ed. Engl.*, 1983, **22**, 113–134.
32 B. Krebs and H.-U. Hürter, *Angew. Chem., Int. Ed. Engl.*, 1980, **19**, 481–482.
33 H. Diercks and B. Krebs, *Angew. Chem., Int. Ed. Engl.*, 1977, **16**, 313.
34 O. Conrad, C. Jansen and B. Krebs, *Angew. Chem.*, 1998, **110**, 3396–3407.
35 D.-Z. Li, H. Bai, T. Ou, Q. Chen, H.-J. Zhai and S.-D. Li, *J. Chem. Phys.*, 2015, **142**, 014302.
36 X.-Y. Tang, Z.-H. Cui, C.-B. Shao and Y.-H. Ding, *Int. J. Quantum Chem.*, 2012, **112**, 1299–1306.
37 W.-Z. Yao, J.-C. Guo, H.-G. Lu and S.-D. Li, *Int. J. Quantum Chem.*, 2010, **110**, 2689–2696.
38 L.-J. Zhao, H.-G. Xu, G. Feng, P. Wang, X.-L. Xu and W.-J. Zheng, *Phys. Chem. Chem. Phys.*, 2016, **18**, 6175–6181.
39 H.-G. Xu, Z.-G. Zhang, Y. Feng, J. Yuan, Y. Zhao and W. Zheng, *Chem. Phys. Lett.*, 2010, **487**, 204–208.
40 A. D. Becke, *J. Chem. Phys.*, 1993, **98**, 5648–5652.
41 C. Lee, W. Yang and R. G. Parr, *Phys. Rev. B: Condens. Matter Mater. Phys.*, 1988, **37**, 785–789.
42 R. A. Kendall, T. H. Dunning and R. J. Harrison, *J. Chem. Phys.*, 1992, **96**, 6796–6806.
43 N. B. da Costa, R. O. Freire, A. M. Simas and G. B. Rocha, *J. Phys. Chem. A*, 2007, **111**, 5015–5018.
44 M. J. Frisch, G. W. Trucks, H. B. Schlegel, G. E. Scuseria, M. A. Robb, J. R. Cheeseman, G. Scalmani, V. Barone, B. Mennucci, G. A. Petersson, H. Nakatsuji, M. Caricato, X. Li, H. P. Hratchian, A. F. Izmaylov, J. Bloino, G. Zheng, J. L. Sonnenberg, M. Hada, M. Ehara, K. Toyota, R. Fukuda, J. Hasegawa, M. Ishida, T. Nakajima, Y. Honda, O. Kitao, H. Nakai, T. Vreven, J. A. Montgomery Jr., J. E. Peralta, F. Ogliaro, M. J. Bearpark, J. Heyd, E. N. Brothers, K. N. Kudin, V. N. Staroverov, R. Kobayashi, J. Normand, K. Raghavachari, A. P. Rendell, J. C. Burant, S. S. Iyengar, J. Tomasi, M. Cossi, N. Rega, N. J. Millam, M. Klene, J. E. Knox, J. B. Cross, V. Bakken, C. Adamo, J. Jaramillo, R. Gomperts, R. E. Stratmann, O. Yazyev, A. J. Austin, R. Cammi, C. Pomelli, J. W. Ochterski, R. L. Martin, K. Morokuma, V. G. Zakrzewski, G. A. Voth, P. Salvador, J. J. Dannenberg, S. Dapprich, A. D. Daniels, Ö. Farkas, J. B. Foresman, J. V. Ortiz, J. Cioslowski and D. J. Fox, *Gaussian 09, revision D.01*, Gaussian, Inc., Wallingford, CT, USA, 2009.
45 F. Holka, M. Urban, P. Neogrády and J. Paldus, *J. Chem. Phys.*, 2014, **141**, 214303.
46 J. Čížek, *Advances in Chemical Physics*, John Wiley & Sons, Inc., 2007, pp. 35–89.
47 G. E. Scuseria and H. F. Schaefer, *J. Chem. Phys.*, 1989, **90**, 3700–3703.
48 H.-J. Werner, P. J. Knowles, G. Knizia, F. R. Manby, M. Schütz, P. Celani, T. Korona, R. Lindh, A. Mitrushenkov, G. Rauhut, K. R. Shamasundar, T. B. Adler, R. D. Amos, A. Bernhardsson, A. Berning, D. L. Cooper, M. J. O. Deegan, A. J. Dobbyn, F. Eckert, E. Goll, C. Hampel, A. Hesselmann, G. Hetzer, T. Hrenar, G. Jansen, C. Köppl, Y. Liu, A. W. Lloyd, R. A. Mata, A. J. May, S. J. McNicholas, W. Meyer, M. E. Mura, A. Nicklass, D. P. O'Neill, P. Palmieri, D. Peng, K. Pflüger, R. Pitzer, M. Reiher, T. Shiozaki, H. Stoll, A. J. Stone, R. Tarroni, T. Thorsteinsson and M. Wang, *MOLPRO, version2012.1, a package of ab initio programs*, http://www.molpro.net.
49 E. D. Glendening, J. K. Badenhoop, A. E. Reed, J. E. Carpenter, J. A. Bohmann, C. M. Morales and F. Weinhold, *NBO 5.0*, Theoretical Chemistry Institute, University of Wisconsin, Madison, 2001.
50 J. Akola, M. Manninen, H. Häkkinen, U. Landman, X. Li and L.-S. Wang, *Phys. Rev. B: Condens. Matter Mater. Phys.*, 1999, **60**, R11297–R11300.
51 D. J. Tozer and N. C. Handy, *J. Chem. Phys.*, 1998, **109**, 10180–10189.
52 V. A. Mozhayskiy and A. I. Krylov, *ezSpectrum*, see http://iopenshell.usc.edu/downloads.
53 A. Jenouvrier and B. Pascat, *Can. J. Phys.*, 2011, **59**, 1851–1861.
54 A. Jenouvrier and B. Pascat, *Can. J. Phys.*, 1981, **59**, 1862.
55 H.-J. Zhai, L.-M. Wang, S.-D. Li and L.-S. Wang, *J. Phys. Chem. A*, 2007, **111**, 1030–1035.

 This journal is © The Royal Society of Chemistry and the Centre National de la Recherche Scientifique 2018